# ACTUATOR PLACEMENT VIA GENETIC ALGORITHM FOR AIRCRAFT MORPHING

*Final Summary of Research*
*conducted under NASA Grant NAG 1-2262*


William A. Crossley, Associate Professor
Andrea M. Cook, Graduate Research Assistant

School of Aeronautics and Astronautics
Purdue University
1282 Grissom Hall
West Lafayette, Indiana 49707-1282

# ACTUATOR PLACEMENT VIA GENETIC ALGORITHM FOR AIRCRAFT MORPHING

*Final Summary of Research*
*conducted under NASA Grant NAG 1-2262*

Submitted by:
William A. Crossley, Assistant Professor
Andrea M. Cook, Graduate Research Assistant
School of Aeronautics and Astronautics, Purdue University
1282 Grissom Hall, West Lafayette, IN 47907-1282

## ABSTRACT

This research continued work that began under the support of NASA Grant NAG 1-2119. The focus of this effort was to continue investigations of Genetic Algorithm (GA) approaches that could be used to solve an actuator placement problem by treating this as a discrete optimization problem. In these efforts, the actuators are assumed to be "smart" devices that change the aerodynamic shape of an aircraft wing to alter the flow past the wing, and, as a result, provide aerodynamic moments that could provide flight control. The earlier work investigated issued for the problem statement, developed the appropriate actuator modeling, recognized the importance of symmetry for this problem, modified the aerodynamic analysis routine for more efficient use with the genetic algorithm, and began a problem size study to measure the impact of increasing problem complexity. The research discussed in this final summary further investigated the problem statement to provide a "combined moment" problem statement to simultaneously address roll, pitch and yaw. Investigations of problem size using this new problem statement provided insight into performance of the GA as the number of possible actuator locations increased. Where previous investigations utilized a simple wing model to develop the GA approach for actuator placement, this research culminated with application of the GA approach to a high-altitude unmanned aerial vehicle concept to demonstrate that the approach is valid for an aircraft configuration.

## INTRODUCTION

Interest in using smart and adaptive materials and structures to improve aircraft performance has been encouraged by research programs like NASA's Aircraft Morphing Program.[1] This research supports multidisciplinary design optimization efforts for aircraft morphing by investigating how genetic algorithms can be used to optimize the placement and number of discrete "smart actuators" for aircraft flight control. These smart actuators may eliminate the need for conventional control surfaces by changing the aerodynamic characteristics of lifting surfaces to produce pitching, rolling, and yawing moments.[2] Several concepts have been proposed for these smart actuator devices. These concepts include flexible/inflatable skins, piezoelectric actuators in composite laminates, shape memory alloys, and synthetic zero-mass jets driven by vibrating smart membranes.[3] Eliminating conventional control surfaces has many benefits, including the reduction of leakage and protuberance drag, aerodynamic noise, and radar cross-section. In order for smart actuators to be successful in aircraft maneuverability, the proper placement of actuators is vital. Reducing the required number of these actuators to perform flight maneuvers will likely reduce the cost and / or power required for control of the aircraft.

The effort described in this report had several goals, which built upon previous research.[4,5] The first goal was to demonstrate a single problem statement that will minimize the total number of unique actuators needed to provide uncoupled control moments about all three body axes corresponding to pitch, roll, and yaw maneuvers. This problem statement encourages actuator placements that share active actuator locations (e.g. one or more of the actuators used for pitch is also used for roll and/or yaw). The initial problem statement investigations used a simple, unswept, untapered wing with 16 possible actuator locations as the aircraft model; an important goal was to investigate the effect of increasing the problem size for models with more than 16 actuator locations. The final goal was to apply the GA technique for actuator placement to an aircraft configuration to demonstrate that the approach was not dependent upon the simple wing model.

# METHODS

## THE GENETIC ALGORITHM

The Genetic Algorithm (GA) is a computational representation of natural selection and reproduction, observed in biological populations.[6] The analogy between "survival-of-the-fittest" and optimization has lead to many application of GAs for optimal design. This approach is becoming an accepted technique to solve many difficult problems in engineering and other fields.

The GA is not a numerical optimization method; it searches with a population of points that evolves over several generations, rather than from point-to-point over successive steps. Further, the GA does not require gradient information to conduct its search, and the search itself uses probabilistic techniques to move from one generation to the next. Finally, the GA normally uses a coding of the design parameter, of "genes," to form a "chromosome" that represents each individual design. This coding allows for a combination of discrete and continuous design variables. More details about the genetic algorithm can be found in several textbooks, such as Ref. 6.

For this problem, the chromosomes are coded as a binary string of 1s and 0s. This allows each possible actuator location to correspond to one bit in the chromosome string, where a 1 represents an active or "on" actuator, and a 0 represents an inactive or "off" actuator. This binary coding makes the GA well suited to the discrete optimization approach to the actuator placement problem.

The GA employed here uses uniform crossover to produce the next generation of designs. This crossover routine proceeds through each bit of the parents' chromosomes and determines at random whether the bit will be swapped to produce the child designs. Previous work[4] indicated that uniform crossover performed as well or better than single-point crossover in both the result quality and the computational time required to reach a stopping criterion, so this basic approach was employed here, as well. For this work, the GA stops running if the best design in the population does not change for five consecutive generations.

## SIMPLE WING MODEL AND AERODYNAMIC ANALYSIS

To begin investigations of the actuator placement problem, a simple wing was modeled with 16 possible actuator locations. The wing has a NACA 0015 airfoil section and is untapered and unswept. This model has an aspect ratio of 8. The wing model shown in Fig. 1 appears in both an isometric view and "unwrapped" about the leading edge with the 16 possible actuator locations labeled. In the isometric view, the eight upper surface actuator locations are shaded and labeled with their corresponding numbers. These locations for possible actuator placements were chosen to provide large moment arms, which should allow the actuators to generate control moments in all three axes.

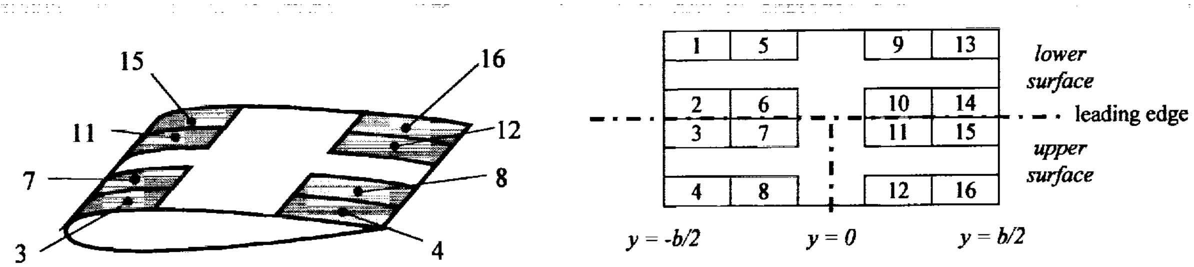


**Fig. 1 Simple NACA 0015 section wing model isometric view (left) and "unwrapped" wing model (right) with discrete actuator locations indicated.**

PMARC, a 3-D panel code, is used to predict the aerodynamic force and moment coefficients for each design.[7] The wing model is divided into 2400 panels: 20 spanwise by 120 chordwise (60 on the upper surface and 60 on the lower surface). In order to allow for equally sized actuators, the panels are all equally spaced over the surface of the wing. In addition, a rigid wake is attached to the trailing edge of the wing. This wake contains 240 panels with cosine spacing. The smallest panels are located closest to the wing to ensure the most accurate calculation possible.

To provide aircraft flight control, the actuators must generate pitching, rolling and yawing moments. These moments are defined using the body axis centered definitions consistent with the PMARC code. These body axes and corresponding sign conventions for the moments appear in Fig. 2. Rolling moment is denoted as $c_l$; pitching moment, $c_m$; and yawing moment, $c_n$.

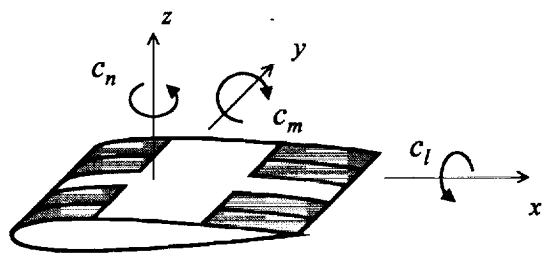


**Fig. 2 Body axes and aerodynamic moment sign conventions.**

## ACTUATOR MODELING

Using PMARC as the aerodynamic analysis program requires that the wing be covered with panels. The actuator locations are "patches" or areas that encompass several aerodynamic panels. For example, each actuator location shown in Fig. 1 includes 80 total panels and four in the spanwise direction and 20 in the chordwise direction.

An active, or "on", actuator is modeled by imposing positive normal velocities (blowing) and negative normal velocities (suction) in the area defined by the actuator. By using an equal number of panels with blowing and suction, the actuator model changes the flow past the wing without adding mass to the flow. Nearly any practical smart actuator system can be represented in PMARC using blowing and suction, if the PMARC model has a similar aerodynamic effect on the flow to the actual device. Fig. 3 shows the relative normal velocities for an active actuator in PMARC as used in this research. Here, this actuator area has two spanwise panels and 10 chordwise panels.

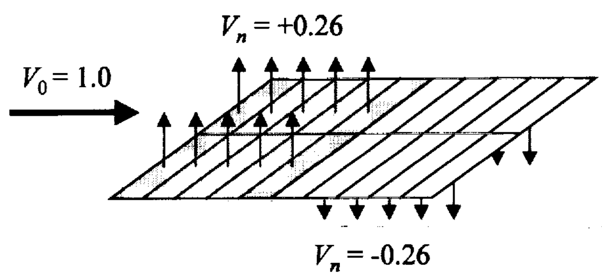


**Fig. 3 PMARC model of active actuator with positive and negative normal velocities.**

With the lack of reliable aerodynamic data for envisioned smart actuator devices, the actuators for this effort are modeled in PMARC to have a similar effect as a conventional control surface on a NACA 0015 airfoil. The pressure coefficient distribution of a conventional flap deflected 15°, as calculated by XFOIL,[8] were used for comparison. Fig. 4 shows the $c_p$ curves at the trailing edge of a NACA 0015 airfoil. The left plot is for a chordwise section through an active actuator on the wing modeled in PMARC, and the right plot is for a conventional flap deflected 15° modeled by XFOIL.

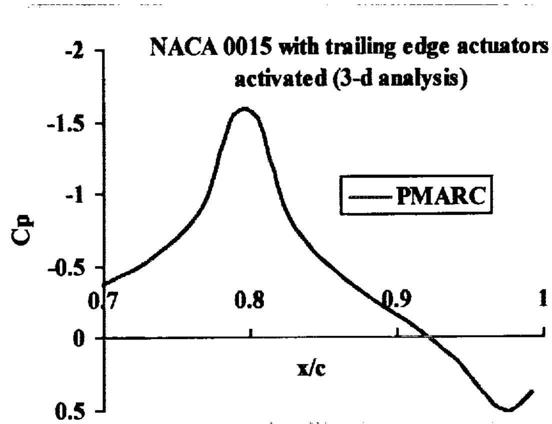


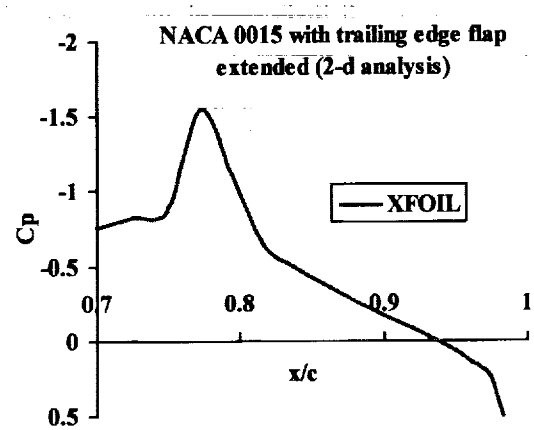


**Fig. 4 Pressure coefficient plots for NACA 0015 wing modeled with active trailing edge actuators (left) and NACA 0015 airfoil with conventional trailing edge flap (right).**

The intent here was to qualitatively match the suction/blowing actuator model in PMARC with the XFOIL $c_p$ distribution. An inverse design approach, using the normal velocity magnitudes as design variables, could increase the accuracy of this match. Additionally, the comparison of the PMARC actuator model was made with a conventional trailing edge flap, because accurate $c_p$ data about smart effectors is not readily available at present.

During the previous research effort, PMARC was modified to improve how it is used in the genetic algorithm-based approach for actuator placement.[5] The major modification involved replacing the linear system of equations solution routine. Because the actuator effects are modeled through surface velocities in the GA-based approach for actuator placement, the large matrix of influence coefficients remains the same for all individual placement designs in the GA population. On the first call to PMARC for analysis, the influence coefficient matrix is constructed, inverted and stored. Every subsequent call to PMARC can solve for the doublet strengths by forward multiplying the inverted coefficient matrix by the velocity vector. This approach greatly increases the computational time of the first call to PMARC, but subsequent calls using forward multiplication are several orders of magnitude faster than the original PMARC. For the thousands of evaluations required by the GA-based approach, this markedly reduced the elapsed time needed to generate actuator placement designs.

## RESEARCH RESULTS

### COMBINED MOMENT PROBLEM STATEMENT

Previous work illustrated that the use of maneuver symmetry in the problem statement dramatically reduced the computational time and reduces the number of infeasible actuator placements in the design space.[4] The concept of maneuver symmetry is based on the observation that for uncoupled maneuvers, "on" actuators must be located with some line of symmetry. For example, an uncoupled pitching maneuver requires a pitching moment without any moments in roll or yaw; actuator placements that are symmetric between the right and left sides of the aircraft produce this uncoupled maneuver. The investigation to combine roll, pitch, and yaw in a single problem statement also uses symmetry so that each bit in the binary chromosome represents two possible actuator locations, one on either side of the appropriate axis of symmetry. The axes of symmetry for pitch, roll, and yaw are shown in Fig. 5, using the 16-actuator locations described previously.

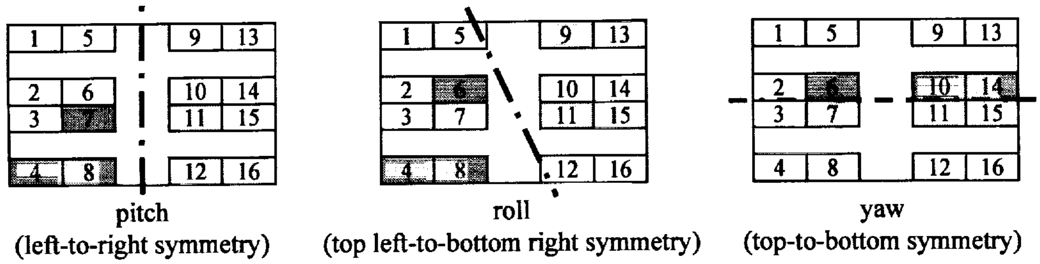


**Fig. 5 Axes of symmetry for pitch, roll, and yaw.**

With this symmetry arrangement, eight bits can represent all sixteen possible actuator locations. For example, the eight bits used for the pitch maneuver actuator placement represent locations 1 through 8. The chromosome corresponding to the actuator placement shown in Fig. 5 for pitch is "00010011", which indicates that locations 4, 7, and 8 are "on" actuators (these are shaded in Fig. 5). Through the left-to-right symmetry definition, this eight-bit string also indicates that locations 16, 11, and 12 are "on" actuators (these are also shaded).

In a similar manner, the eight-bit string for the roll maneuver actuator placement represents locations 1-8. The roll example depicted in Fig. 5 has the chromosome: "00010101" indicating locations 4, 6 and 8 are "on" actuators; using the top left to bottom right symmetry, actuator locations 13, 11, and 9 are also "on". For the yaw maneuver, the eight-bit string corresponds to locations 1, 2, 5, 6, 9, 10, 13, and 14. In Fig. 5, the chromosome "00010101" corresponds to the yaw example. This turns on actuators at locations 6, 10 and 14. By symmetry, actuator locations 7, 11, and 15 are also turned on.

To handle the combined moment problem, the design chromosomes are encoded as two-dimensional arrays for convenience. The first row (8 bits in the 16-actuator location problem) of the array represents the actuators to achieve a pitching moment. The second and third rows represent the actuators for a rolling and yawing moment, respectively. The chromosome array corresponding to the maneuver examples depicted in Fig. 5 is

$$\begin{array}{cl} \begin{bmatrix} 00010011 \\ 00010101 \\ 00010101 \end{bmatrix} & \begin{array}{l} \textit{pitch} \\ \textit{roll} \\ \textit{yaw} \end{array} \end{array} \tag{1}$$

For this problem, the objective is to minimize the total number of "on" actuator locations needed to produce uncoupled roll, pitch, and yaw moments. The objective function is posed as:

minimize $$\phi = \sum_{i=1}^{l} \max\left(a_{1i}, a_{2i}, a_{3i}\right) \tag{2}$$

where $a_{ni}$ is the bit value corresponding to actuator location $i$ from the $n^{\text{th}}$ row of the actuator binary chromosome array, and $l$ is the number of possible actuator locations for each maneuver (here, $l$ is 16). Because $a_{ni}$ can only be "1" or "0" to represent on or off actuator locations, the max($a_{1i}$, $a_{2i}$, $a_{3i}$) term equals one if at least one of the maneuvers uses an "on" actuator at location $i$ and equals zero only if all three maneuvers have "off" actuators at location $i$.

To illustrate how the objective function is computed, consider the actuator placement design depicted in Fig. 5 and represented by the chromosome in Eqn. 1. Several "on" actuator locations are shared among the three maneuver conditions; these shared locations only contribute a value of 1 to the objective function. For example, location 4 is shared by the pitch and roll maneuvers. Table 1, below, attempts to display this further. In the table, there are rows for the three maneuvers and columns for each actuator location. "On" actuators for each maneuver are indicated with an "×" in the table. The last row provides the max($a_{1i}$, $a_{2i}$, $a_{3i}$) value, so a sum of this last row provides the objective function. For this design, the objective function, $\phi$, equals 12.

**Table 1 Example actuator locations used for pitch, roll, and yaw maneuvers.**

| | 1 | 2 | 3 | 4 | 5 | 6 | 7 | 8 | 9 | 10 | 11 | 12 | 13 | 14 | 15 | 16 |
|---|---|---|---|---|---|---|---|---|---|---|---|---|---|---|---|---|
| Pitch | | | | × | | | × | × | | | × | × | | | | × |
| Roll | | | | × | | × | | × | × | | × | | × | | | |
| Yaw | | | | | | × | × | | | × | × | | | × | × | |
| $\max(a_{1i}, a_{2i}, a_{3i})$ | 0 | 0 | 0 | 1 | 0 | 1 | 1 | 1 | 1 | 1 | 1 | 1 | 1 | 1 | 1 | 1 |

The placement design presented by Fig. 5 provides for moments in one direction about each body axis, which correspond to only three possible maneuvers. To provide all six desired maneuvers, the "mirror images" of the example actuator placement designs depicted in Fig. 5 are required. Below, Fig. 6 displays both the initial actuator placement design to allow pitch up, roll left, and yaw right and the mirror image actuator placements to allow pitch down, roll right, and yaw left.

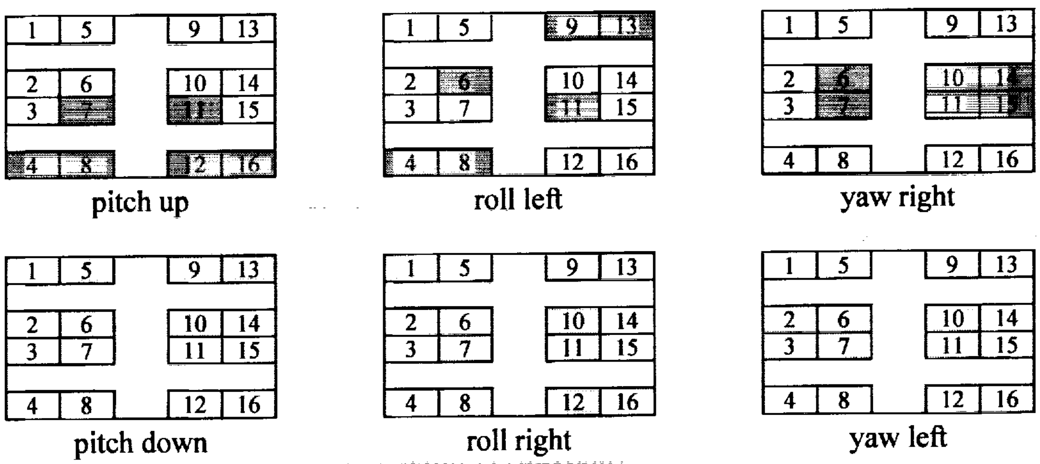


**Fig. 6 Actuator placement design (top) and mirror image placements (bottom) for all six maneuvers.**

While the objective function for this design is 12, based upon Eqn. 2; all 16 actuator locations are needed to perform the complete set of six maneuvers. However, using only the pitch down, roll left, yaw right actuator locations to describe the objective function makes this a better design than a design that would require all 16 actuators to be used for any of the maneuvers. As the genetic algorithm progresses through subsequent generations, the selection operator encourages survival of designs using the fewest number of actuators.

Problem constraints describe the uncoupled maneuver conditions. The development of a control strategy, most likely including pitch, roll, and yaw rates, would set the limiting maneuver values for more fully developed, practical applications. For this research, the values of the constraints were determined by computing the moment coefficients when actuators located in the same place as conventional control surfaces were active. For example, the pitching moment coefficient was determined by computing the coefficient associated with turning "on" the actuator devices located on the trailing edge that correspond to conventional trailing edge flap locations. The models used to set the pitch, roll, and yaw moment constraint limits appear in Fig. 7. Multiplying the values of $c_m$, $c_l$, and $c_n$ computed for these placements by 0.985 determined the limit values for these moments.

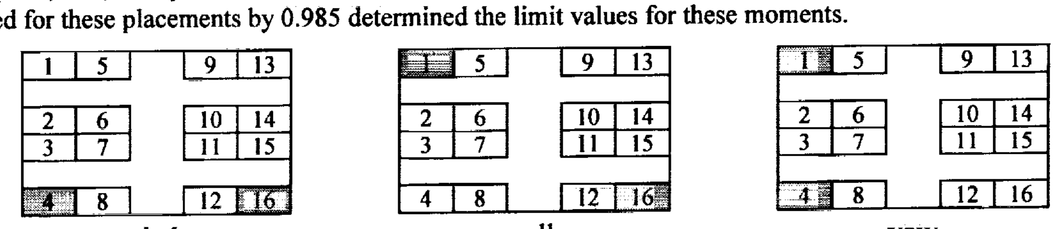


**Fig. 7 Actuator placements used to set constraint limits.**

The constraint functions ensure that a minimum limiting moment can be achieved about one axis while the moments about the other axes are very small. Like the chromosome array, an array representation of the constraint functions was developed for convenience. The first row of the chromosome matrix represents the pitch maneuver; the second, roll; and the third, yaw. These are posed so that the constraint function values are negative when satisfied ($g_{ij} \leq 0$).

$$g_{11} = 1 - \frac{c_m}{0.0279} \qquad g_{12} = \frac{|c_n|}{0.001} - 1 \qquad g_{13} = \frac{|c_l|}{0.001} - 1 \tag{3}$$

$$g_{21} = +\frac{c_l}{1\ 141} \qquad g_{22} = \frac{|c_n|}{0.001} - 1 \qquad g_{23} = \frac{|c_m|}{0.001} - 1 \tag{4}$$

$$g_{31} = -\frac{c_m}{1\ 1140} \qquad g_{32} = \frac{|c_m|}{0.001} - 1 \qquad g_{33} = \frac{|c_l|}{0.001} - 1 \tag{5}$$

Constraint $g_{11}$ ensures that the pitching moment is 0.0279 or greater, which corresponds to a minimum magnitude for $c_m$. The other constraints in the first row, $g_{12}$ and $g_{13}$, ensure that the magnitude of the yawing ($c_n$) and rolling ($c_l$) moments are equal or less than 0.001 to represent an uncoupled pitching moment. The actuator placement designs represented by the second and third rows of the chromosome are subject to similar uncoupled rolling and yawing constraints. In these cases, the rolling moment must be less than -0.0409, and the yawing moment must be greater than 0.0042.

The GA uses only a single fitness function to guide its search. Because of this, the fitness function must include both the objective function and the constraints. Based on previous investigations for actuator placement, the step-linear external penalty function approach incorporates constraint violations for this work. The fitness function, $f$, is

$$\begin{aligned} f &= \phi + \sum_{i=1}^{3}\sum_{j=1}^{3}\left(r_0 \zeta_{ij} + r_{ij}\max[0, g_{ij}]\right) \\ \zeta_{ij} &= \begin{cases} 0 & g_{ij} \leq 0 \\ 1 & g_{ij} > 0 \end{cases} \end{aligned} \tag{6}$$

The penalty multiplier coefficients, $r_0$ and $r_{ij}$, are chosen such that the penalty terms are on the same order of magnitude as the objective function when the constraints are violated.

This problem statement addresses three uncoupled maneuvers; however, there is an additional aspect of symmetry that is required to allow a fully maneuverable aircraft about all three body axes. The constraints presented in Eqns. 3, 4, and 5 result in "on" actuator location designs corresponding to a nose up pitch ($c_m \geq 0.0279$), a roll to the right (i.e. left wing up, $c_l \leq -0.0409$), and a yaw to the left ($c_n \geq 0.0042$). In addition, an aircraft would also be required to pitch down, roll left, and yaw right, which may require additional "on" actuator locations using the mirror image placements as described previously.

**PROBLEM SIZE STUDIES**

The first investigations of the combined moment problem for actuator placement used the 16-actuator wing model discussed in the previous text. This simple model allowed for comparatively short run times and provided results that were easy to interpret. Effects of problem size were investigated by using wing models with 32 and 64 possible actuator locations. These larger problem sizes illustrated the advantages of a genetic algorithm-based approach for actuator placement over an enumerative search of the design space. Five runs were conducted for each problem, which allowed some assessment of the GA's consistency when solving these actuator placement problems. All of the GA runs used population size and mutation rate guidelines based upon chromosome length.[9]

### 16-ACTUATOR LOCATION PROBLEM

To find placement designs for the 16-location problem, the GA was run using a population size of 96 and a mutation rate of 0.0054. A placement design resulting from one of the five GA runs for the 16-actuator location problem appears in Fig. 8. The composite design, illustrating all the necessary "on" actuator locations appears at the top of the figure, and the corresponding pitch, roll, and yaw schemes are shown at the bottom. For this placement design, actuator location 16 is shared by the pitch and roll maneuvers, and the resulting fitness function value is 5.0. The design shown produces moments for pitch up, roll right, and yaw left maneuvers, based upon the design constraints. The pitching moment for this design is 0.02832, the rolling moment is -0.04162, and the yawing moment is 0.00835. For this design to produce pitch down, roll left, and yaw right maneuvers, the actuator locations on the opposite sides of the axes of symmetry are needed. These opposite actuators are 13, 14, and 15; therefore, to perform all desired maneuvers, eight actuator locations are needed. The yaw maneuver placement shown here provides a value of $c_n$ that clearly exceeds the limit value set by using placements of "on" actuators that mimic traditional control surface locations. This result suggests that the GA can often generate designs not intuitive or obvious to a designer.

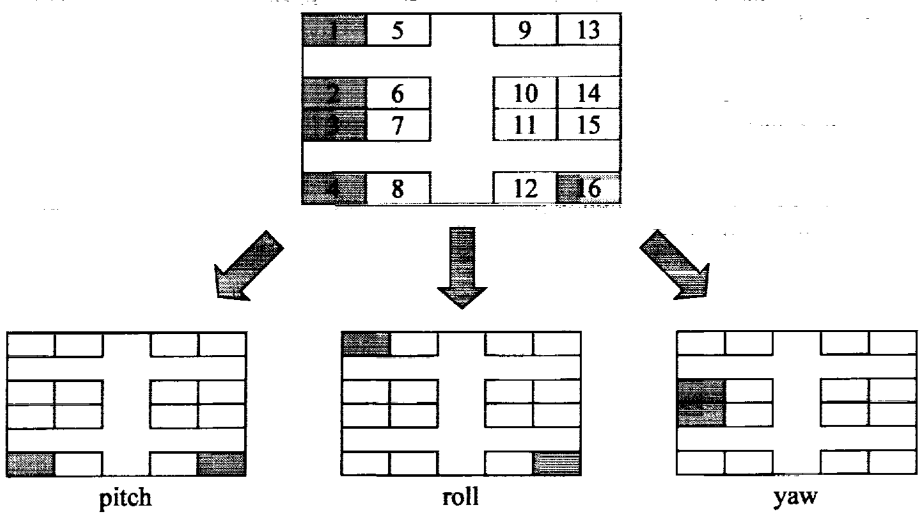


**Fig. 8 Combined moment problem result showing "on" actuator locations indicated by the chromosome (top) and the corresponding pitch, roll and yaw maneuver "on" locations (bottom), 16 actuator locations.**

Fitness history plots for the run to generate the above placement design appear in Fig. 9. These plots show the minimum (best) fitness value of any individual in each generation, the maximum (worst) fitness value of any individual in each generation, and the average value of all individuals in each generation. The plot of the best individual design (minimum fitness) in each generation is expanded on a different fitness scale to show the improvement in the best design as the GA progresses towards the stopping criterion. In addition to the placement design shown in Fig. 8, several different five-actuator designs appear in the final generation of designs, as well as feasible designs with six or more actuators. With this large number of feasible configurations, a designer can apply additional selection criteria to determine the best five-actuator placement design from these designs.

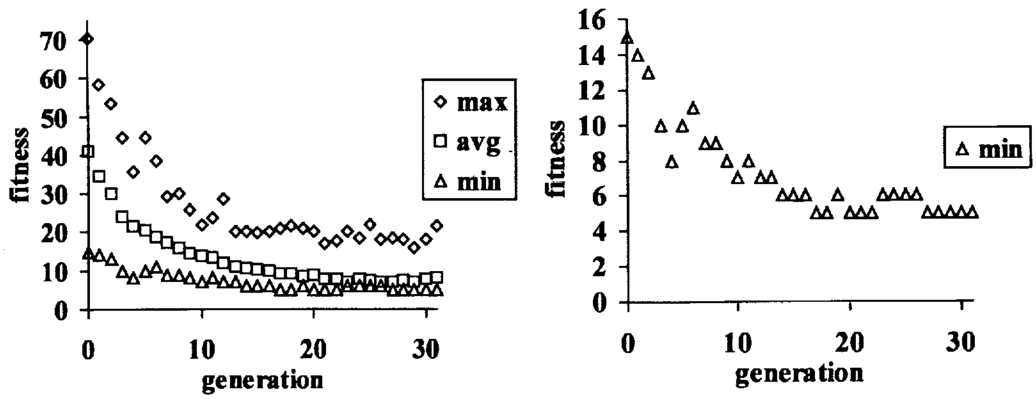


**Fig. 9 Fitness history for 16-actuator location combined moment problem: maximum, average and minimum fitness (left) and minimum fitness only (right).**

The GA run described above required about 24 hours of CPU time on a Sun Ultra-450 computer, which is a non-trivial computational expense. This example run required 31 generations to reach the stopping criterion, but the average number of generations required for all five of the 16-actuator combined moment problems was 23.6. The efficiency of the GA for this problem is apparent when compared to an enumerative search. For the 16-actuator combined moment problem, $2^{24}$ (24 bits, each with two possible values) possible designs exist. Each actuator placement design requires three PMARC analyses to evaluate the three maneuvers, so an enumerative search would use 50,331,648 PMARC analyses. The GA required only 9,216 PMARC analyses to generate several feasible designs for the run depicted in Fig. 9. Computing the GA cost based upon the average number of generations required over the five different runs, this cost is just below 6,800 evaluations.

### 32-ACTUATOR LOCATION PROBLEM

Next, the problem was expanded to include 32 possible actuator locations. Here, the chromosome contained 48 bits; using maneuver symmetry, 16 bits represent placements for each maneuver. Five different runs of the GA were conducted for the 32-location problems. The GA population size and mutation rate were set at 192 and 0.00266, respectively. To create 32 locations, the actuator locations from the 16-location wing model were divided in half chordwise. Using a scheme similar to that of the 16-location wing model, the placement and numbering of the 32 actuators is shown in Fig. 10. The same number of aerodynamic panels is maintained for the PMARC model; now, each actuator location encompasses four spanwise and ten chordwise panels.

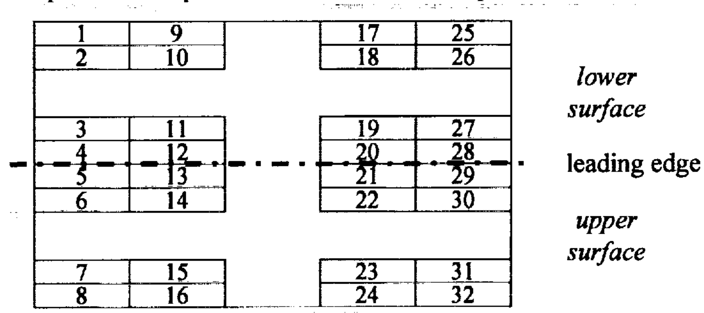


**Fig. 10 Unwrapped wing model with 32 actuator locations.**

The objective function uses the same formula as Eqn. 2, with the exception that here, $l$ is 32. Because each actuator location is smaller than for the 16-location problem, new values of the constraint limits were determined for the 32-location problem by evaluating the aerodynamic moments generated by "on" actuators in locations similar to traditional control surfaces. The locations used to set these limits appear in Fig. 11. With the change in the chordwise dimension of the actuator, the limit values for the desired pitch, roll, and yaw moments are different from those posed for the 16-location problem. The 32-location problem constraints describe an uncoupled pitching moment greater than or equal to 0.0199, an uncoupled rolling moment less than or equal to -0.0299, and an uncoupled yawing moment greater than or equal to 0.00309.

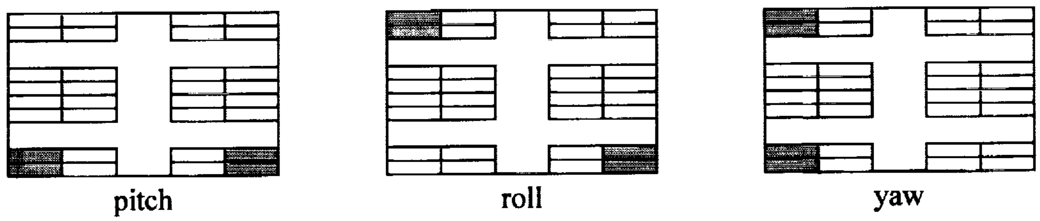


**Fig. 11 Actuator locations used to set moment constraints for 32-location problem.**

Fig. 12 shows a minimum-fitness actuator placement scheme resulting from one of the five GA runs. In this placement design, the roll scheme shares actuators with both pitch and yaw, resulting in an eight-actuator composite scheme that has a fitness value of 8.0. This configuration provides a pitching moment of 0.02869, a rolling moment of -0.03040, and a yawing moment of 0.00804. In order to produce pitch, roll, and yaw moments in both directions, actuators 25 and 28 (see Fig. 10) are necessary.

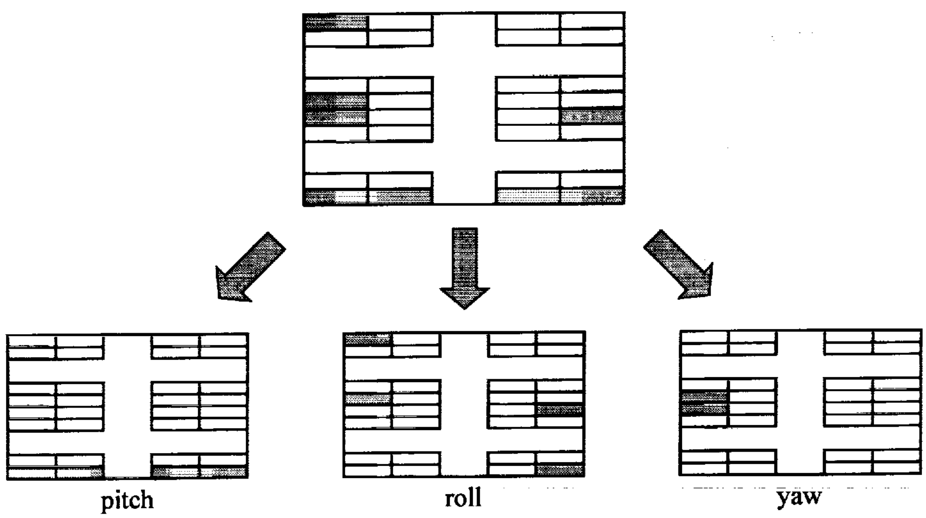


**Fig. 12 Combined moment problem result showing "on" actuator locations indicated by the chromosome (top) and the corresponding pitch, roll and yaw maneuver "on" locations (bottom), 32 actuator locations.**

The GA-generated result shown above creates moment coefficients that satisfy the constraints for this problem, and the final placement design shares actuator locations to minimize the fitness function. In doing so, both the roll and the yaw placements are "non-intuitive" placements. Rather than generating a design with the same "on"-actuator placements as those used to develop the constraint limits, the design in Fig. 12 uses leading edge locations to provide the roll maneuver and the yaw maneuver. In the case of the yaw maneuver, this leading edge actuator scheme far exceeds the limiting value for $c_n$. By sharing the leading edge location for both roll and yaw, the total number of "on" actuator locations is reduced while the constraints are still satisfied.

The fitness history for the 32-actuator problem is similar to that of the 16-actuator problem. Fig. 13 shows these plots for the 32-actuator run that resulted in the design shown in Fig. 12. This run required 27 generations to reach the stopping criterion. The average number of generations required for this problem was 28.4, based on five different runs of the GA. This larger problem required 42 CPU hours, about twice as much CPU time as the 16-actuator problem.

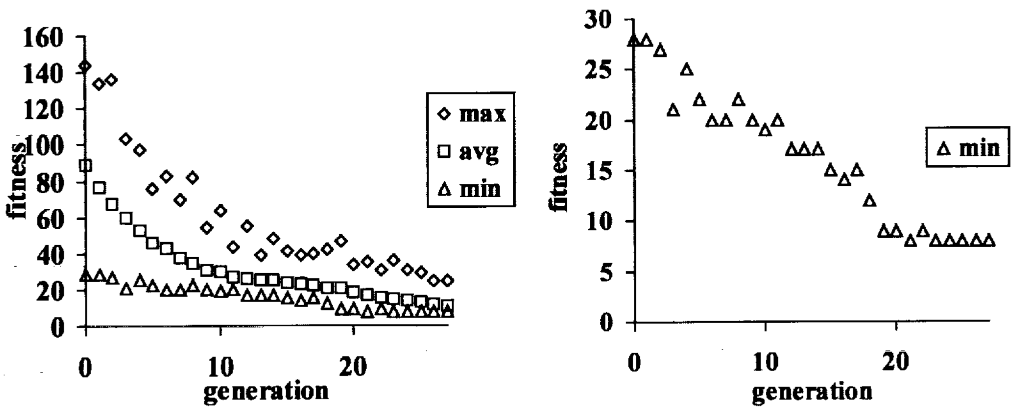


**Fig. 13 Fitness history for 32-actuator location combined moment problem: maximum, average and minimum fitness (left) and minimum fitness only (right).**

Again, the GA required far fewer evaluations than an enumerative search. For the run shown, the GA used only 16,128 PMARC analyses to find several feasible designs; using the average number of generations, the average number of analyses just exceeds 16,934. An enumerative search to evaluate all $2^{48}$ possible designs would require $8.4442\times10^{14}$ PMARC analyses.

**64-ACTUATOR LOCATION PROBLEM**

In the final problem size study using the simple wing geometry, the 32 locations of the previous problem were halved in the spanwise direction to form 64 possible actuator locations. By increasing the complexity of the problem to 64 actuator locations, the benefits of the GA approach are emphasized further. Again, the entire PMARC model retains the original 2,400 aerodynamic panels; for the 64-location problem, each actuator incorporates two spanwise panels and ten chordwise panels.

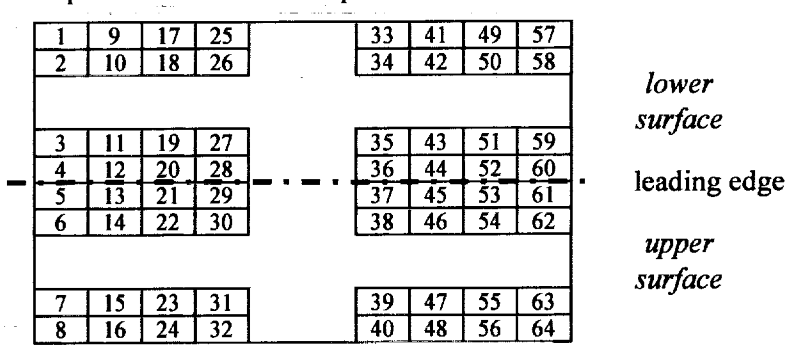


**Fig. 14 Unwrapped wing model with 64 actuator locations.**

Using the maneuver symmetry as in the previous two investigations, 32 bits can be used to represent each of the three maneuvers, so $l$ equals 32 in the objective function (Eqn. 2). The GA ran five times for this problem; each run used a population size of 384 and a mutation rate of 0.00132. Because the possible actuator locations in the 64-location problem have the same chordwise dimension as those of the 32-location problem, the constraint limit values are equal in magnitude of those used in the constraints for the 32-actuator problem. However, for this 64-location problem, the signs of the limiting moments have been changed so that the constraints ask for an uncoupled nose-down pitch with $c_m \le -0.0199$, an uncoupled left roll with $c_l \ge 0.0299$, and an uncoupled left yaw with $c_n \ge 0.00309$. These limit values result from computing $c_m$, $c_l$, and $c_n$ for the placements shown in Fig. 15 and multiplying by 0.985.

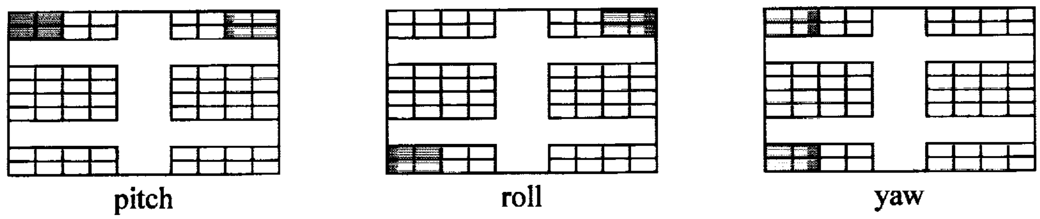


**Fig. 15 Actuator locations used to set moment constraints for 64-location problem.**

All five runs produced "best" designs that used 12 actuator locations to achieve the desired uncoupled pitching, rolling and yawing moments. One of these placement designs is shown in Fig. 16. This particular design provides a pitching moment of -0.02135, a rolling moment with a value of +0.03370, and a yawing moment equal to +0.00450. The mirror image actuator locations at 48, 56, 61, and 64 will allow moments necessary for all six flight-control maneuvers. As for the 32-location problem, minimizing the number of actuators needed for the three maneuvers encourages sharing of actuator locations among the three maneuvers. Here, this has resulted in a somewhat non-intuitive actuator placement that uses three trailing edge and one leading edge device on each side of the wing to achieve the roll moment. This results in a value of $c_l$ that exceeds the constraint limit. One of these leading edge devices is then used in the yaw maneuver, which has a value of $c_n$ exceeding its constraint limit as well.

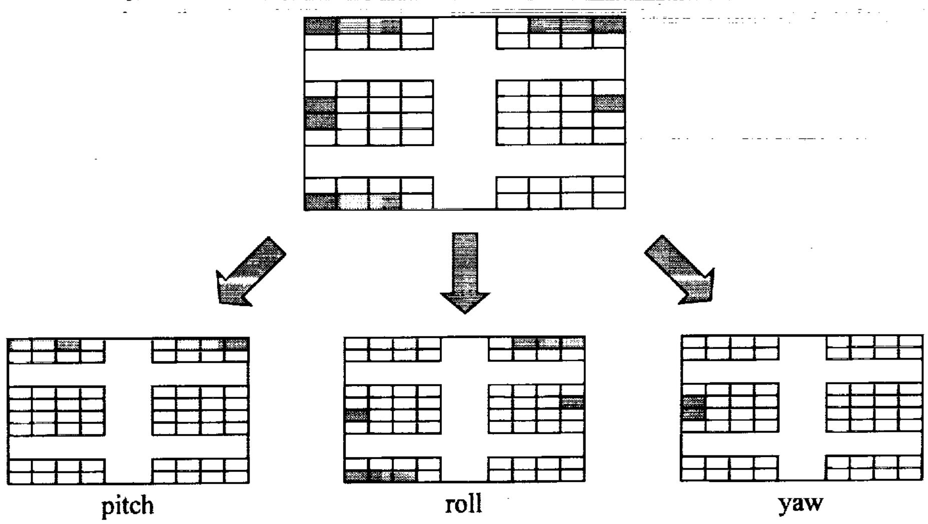


**Fig. 16 Combined moment problem result showing "on" actuator locations indicated by the chromosome (top) and the corresponding pitch, roll and yaw maneuver "on" locations (bottom), 64 actuator locations.**

The run generating the actuator placement shown above required 44 generations to reach the stopping criterion, and a 12-actuator design was first encountered in generation 37. This 64-location problem required nearly 80 hours CPU time, about twice as much as the 32-location problem. The fitness history for this run is shown in Fig. 17. The 64-actuator problem required an average of 45.8 generations, over five total runs. In terms of PMARC analyses, the run corresponding to the design in Fig. 16 required 51,840 analyses; using the average number of generations, the computational cost is nearly 53,914 analyses. With 64 actuator locations and 32 bits representing each of the three maneuver placements, there are $2^{96}$ possible actuator placement designs, so an enumerative search would face the staggering computational cost of $2.3768\times10^{29}$ analyses.

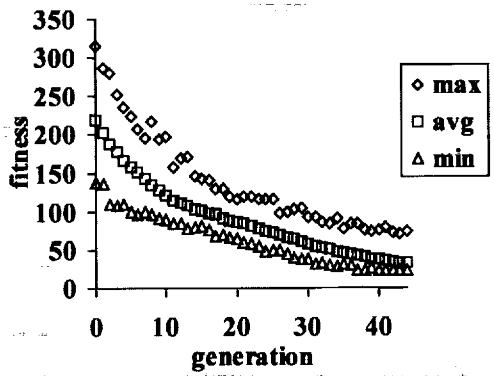


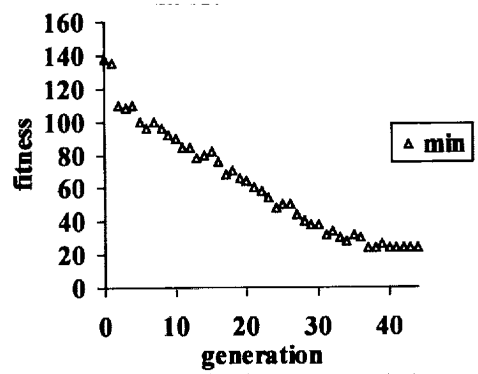


**Fig. 17 Fitness history for 64-actuator location combined moment problem: maximum, average and minimum fitness (left) and minimum fitness only (right).**

Several other feasible actuator placement designs that used different 12-actuator schemes appeared in the final population of the GA. For these alternate placement designs the magnitude of the rolling, pitching and yawing moments varied, but all met the prescribed constraints. A designer could choose from these designs based upon other non-quantitative criteria (e.g. manufacturing concerns) or preferences (e.g. having the highest value yawing moment may be considered more desirable than having the highest possible pitching moment).

## ACTUATOR PLACEMENT ON AIRCRAFT CONCEPT

To illustrate the effectiveness of the GA approach in a more practical aircraft flight control problem, an Unmanned Air Vehicle (UAV) model provided an application for the GA to determine the number and placement of smart actuators necessary to achieve uncoupled pitching, rolling, and yawing moments. The UAV model was adapted from OSCAR, an aircraft designed by Purdue University Aeronautics and Astronautics senior design class students.[10] This aircraft is a high-altitude, long-endurance vehicle that carries a large radar antenna to provide 360° of observation of ground targets. The geometry of the vehicle is a blended wing-body design with a wingspan of about 200 feet. The airfoil shape is cambered, and the wing is twisted 4°. Because of these features, the UAV does not have the same geometric symmetry as the previous wing model; however, the maneuver symmetry (e.g. an uncoupled pitch actuator placement scheme will be left-right symmetric) still exists. The chord of the aircraft's center body is 55 feet long, and the swept wings taper to a chord of about 3 feet. An illustration of the UAV appears in Fig. 18.

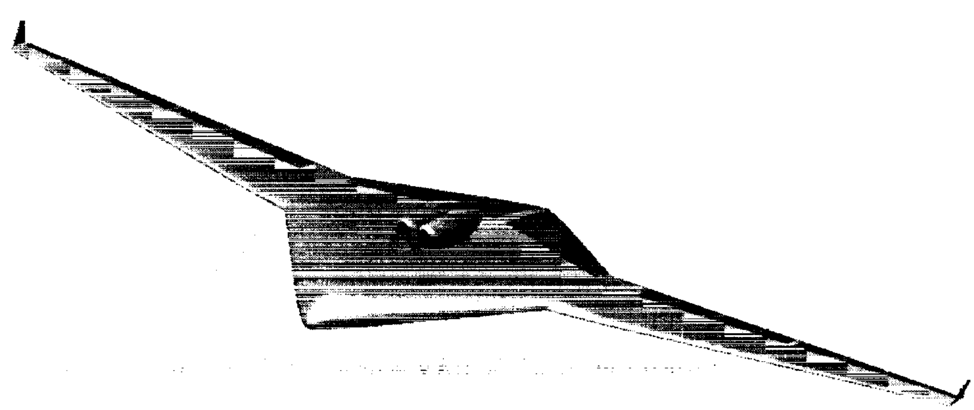

**Fig. 18 High-altitude, long-endurance sensorcraft UAV concept.**

## AIRCRAFT AERODYNAMIC MODEL AND ACTUATOR LOCATIONS

The problem development and statement formulation followed the approach used for the NACA 0015 section wing problems. A PMARC description of the entire UAV was constructed with 2,352 panels; there are 24 panels in the chordwise direction (12 for the lower surface and 12 for the upper surface) and 98 panels in the spanwise direction. As in the wing model, the entire UAV model is divided into evenly spaced segments in the chordwise direction. Because the aircraft has a tapered centerbody and tapered wings, this means that the chordwise dimension changes for each panel boundary. The left and right wing have 30 spanwise panels each.

Thirty-two possible actuator locations were defined near the trailing edge and leading edge, at the root and at the tip, of the wings. Each actuator encompasses four panels in the chordwise direction and five panels in the spanwise direction. This gives the actuators approximately the same aspect ratio as the actuators in the previous NACA 0015 wing model. The actuators defined near the tip of the wing are smaller in area than the actuators defined near the root of the wing, because the size of the aerodynamic panels decrease as the wing tapers. This does not greatly inhibit the effectiveness of the actuators, however, because the moment arm at the tip of the wing is much greater (approximately 100 feet) than at the root of the wing. The locations are not exactly on the leading and trailing edges of the wing to address the concern that an actuator device would not have enough physical space inside the wing at these locations. Fig. 19 shows the 32 possible locations depicted with an "unwrapped" aircraft model using the same basic numbering scheme as employed in the simple wing model. This numbering scheme provided for an easy interface with PMARC.

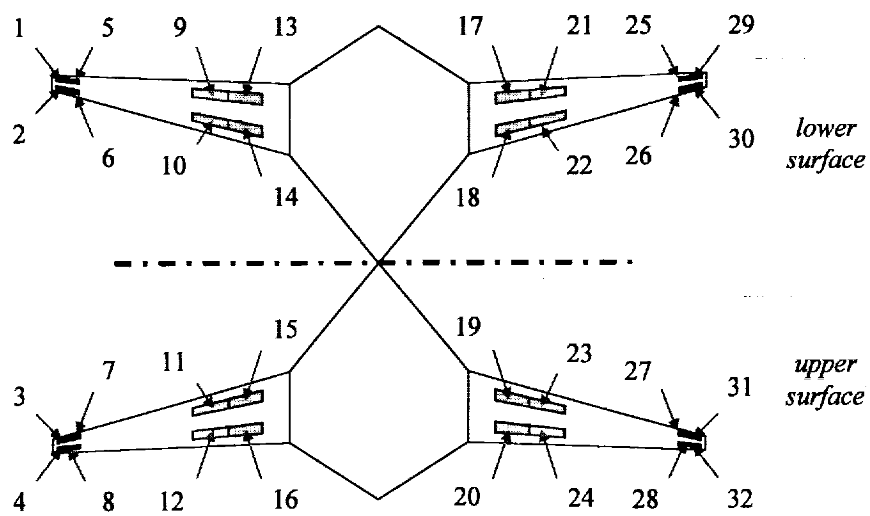


**Fig. 19 Unwrapped UAV model with 32 possible actuator locations identified.**

## ACTUATOR MODELING

The next step in implementing the GA method for actuator placement on the UAV model involved determining the appropriate magnitude of the normal surface velocities to model "on" actuators. To do this, the chordwise pressure coefficient was plotted for the UAV wing for a wing section that passes though an "on" trailing edge actuator when all trailing edge actuators are turned on. The normal (blowing and suction) velocities were modified until the pressure coefficient plot reasonably matched the pressure coefficient plot of the same airfoil with a trailing edge flap as closely as possible. The scheme to model the UAV actuators with normal velocities follows the same upstream blowing, downstream suction scheme presented in Fig. 3. With four chordwise panels per actuator, the UAV actuators have two blowing panels and two suction panels.

From this qualitative process, normal velocities of ±0.10 (relative to the non-dimensional freestream, $V_\infty$=1.0) were selected. Fig. 20 displays these pressure distributions. In the figure, there is a noticeable difference in the "width" of the $C_p$ peaks of the flap and actuators. This difference may be due to the effect of the rest of the UAV model on the three-dimensional PMARC analysis. The PMARC pressure coefficient plot is for a portion of the wing near the middle of the inboard actuator locations. The pressure coefficient plot passing through an outboard actuator location on the UAV wing is similar, except that the peak near the trailing edge of the wing reaches a magnitude of about -0.6.

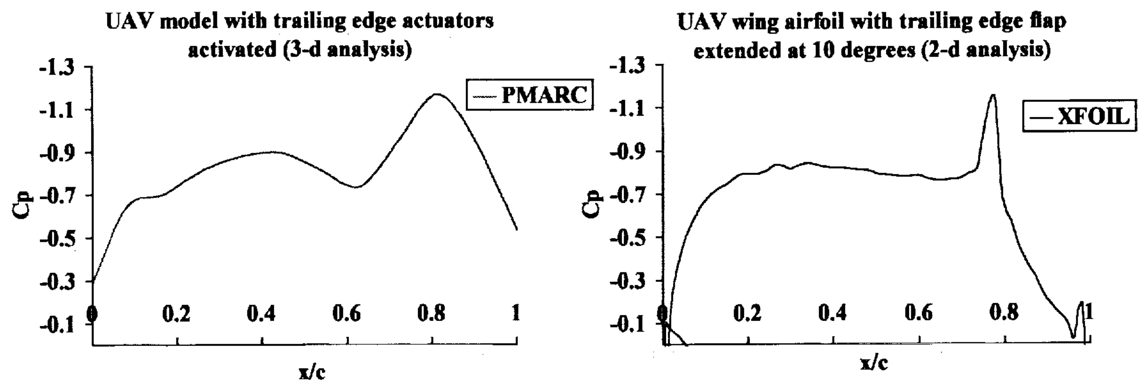


**Fig. 20 Pressure coefficient plots for UAV model with active trailing edge actuators (left) and UAV wing airfoil with conventional trailing edge flap (right).**

## COMBINED MOMENT PROBLEM STATEMENT

The problem statement used for the UAV actuator placement problem follows the problem statement developed using the simple wing model. A chromosome array, like that of Eqn. 1, represents the "on" actuator placements for all three maneuvers. Maintaining the concept of maneuver symmetry for actuator placement shown in Fig. 5, only 16 bits are needed for each row of the chromosome, so the UAV problem needs a total of 48 bits. The goal for the problem is to minimize the number of unique actuator locations that must be turned on to achieve uncoupled pitching, rolling and yawing moments. The objective function for the UAV problem can be described using Eqn. 2, and the fitness function can be described using Eqn. 6.

The constraints also follow the same format used for the wing problem; however, the values of the control moment limits are different. To determine these limit values, PMARC evaluated the moment coefficients for the UAV with "on" actuators in locations near where conventional control surfaces would be located; Fig. 21 displays the placements used to calculate the limiting values for the moment constraints. Maneuver symmetry helped to describe these uncoupled moment actuator placements for computing limiting moment values. For the uncoupled pitch setting, actuators in locations 1, 13, 17 and 29 (see Fig. 19 above) were activated. To compute the rolling moment limit, actuators were "on" in locations 1, 13, 20 and 32. Finally, locations 1, 13, 4 and 16 were turned on to compute the yawing moment constraint value. Again, if specified flight control requirements, such as turn rates, were known, these requirements should be used to set the constraint limit values.

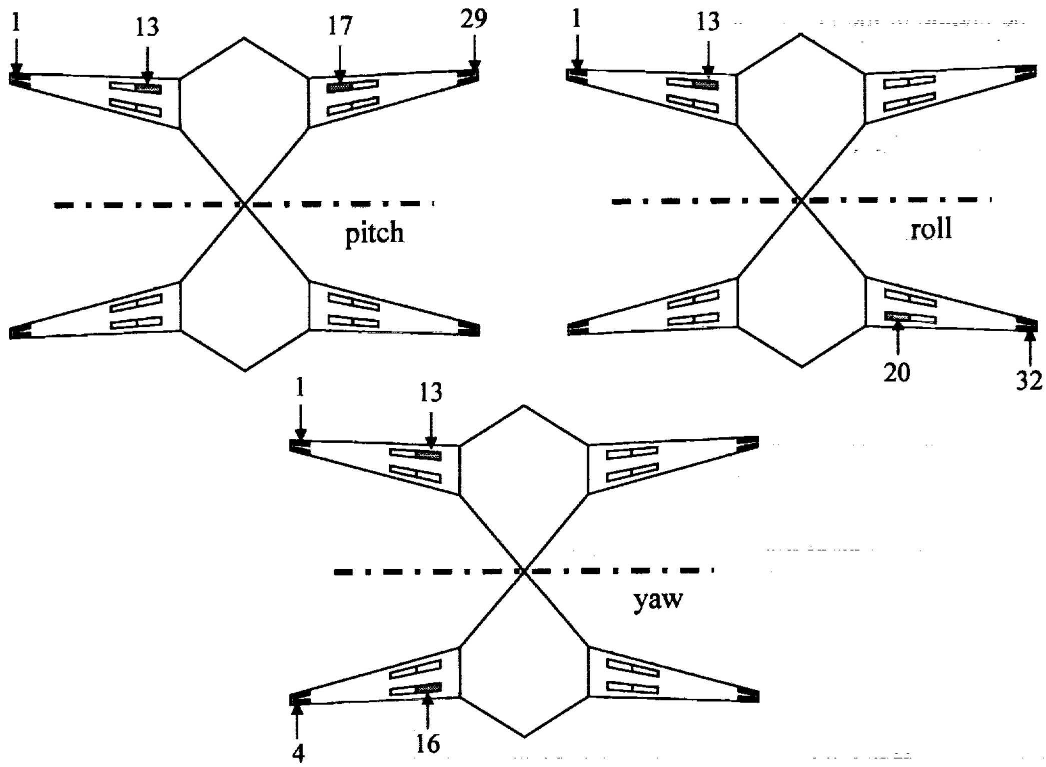


**Fig. 21 Actuator locations to set moment constraints for UAV problem with 32 locations.**

Based on the PMARC results for the three placements shown in Fig. 21, the constraints for the UAV problem are expressed as

$$g_{11} = 1 + \frac{c_m}{0.00190} \qquad g_{12} = \frac{|c_n|}{0.001} - 1 \qquad g_{13} = \frac{|c_l|}{0.001} - 1 \tag{7}$$

$$g_{21} = 1 + \frac{c_l}{0.00164} \qquad g_{11} = \frac{|c_l|}{1d110} - 0 \qquad g_{1} = \frac{|c_m|}{1d110} - 0 \tag{8}$$

$$g_{31} = 1 - \frac{c_n}{0.000167} \qquad g_{32} = \frac{|c_m|}{0.0001} - 1 \qquad g_{33} = \frac{|c_l|}{0.0001} - 1 \tag{9}$$

These constraint equations have similar form to Eqns. 3, 4, and 5, but the constraints for the UAV problem have some notably different values. The magnitudes of the desired uncoupled moments for the UAV are much smaller than for the simple wing. In the equations presented above, the pitching moment is required to be less than or equal to -0.00190; the rolling moment, less than or equal to -0.00164; and the yawing moment, greater than or equal to 0.000167. Further, the uncoupled yaw moment limit that appears in $g_{31}$ for the UAV problem has such a small magnitude, that the limits on the absolute value of pitch and roll were also reduced from those used previously.

## UAV COMBINED MOMENT RESULTS

Five different runs of the GA to generate actuator placement schemes provided an assessment of how effectively actuator placement designs are generated, both in terms of solution quality and computational effort.

With the problem formulation described above, the GA used population size of 192 and a mutation rate of 0.00266 to address the UAV combined moment problem.

An example placement solution for the 32-actuator UAV model is shown in Fig. 22. This UAV actuator placement scheme requires nine total actuators to achieve uncoupled pitch, roll, and yaw. The actuators required to achieve a pitching moment of -0.00300 are located on the lower surface inboard trailing edge on the left and right wings. The actuators used for rolling are located at inboard and outboard locations on the lower surface trailing edge of the right wing and the upper surface trailing edge of the left wing. The rolling moment from these actuators has a value of -0.00193. The yaw actuators are located at inboard and outboard locations on the upper and lower surface right wing trailing edge. The yawing moment produced by these actuators is 0.00017. Because this actuator scheme obtains pitch, roll, and yaw in only three directions (pitch down, roll right, and yaw left), 12 total actuators would be needed in order to obtain these moments in the other three directions (pitch up, roll left, and yaw right).

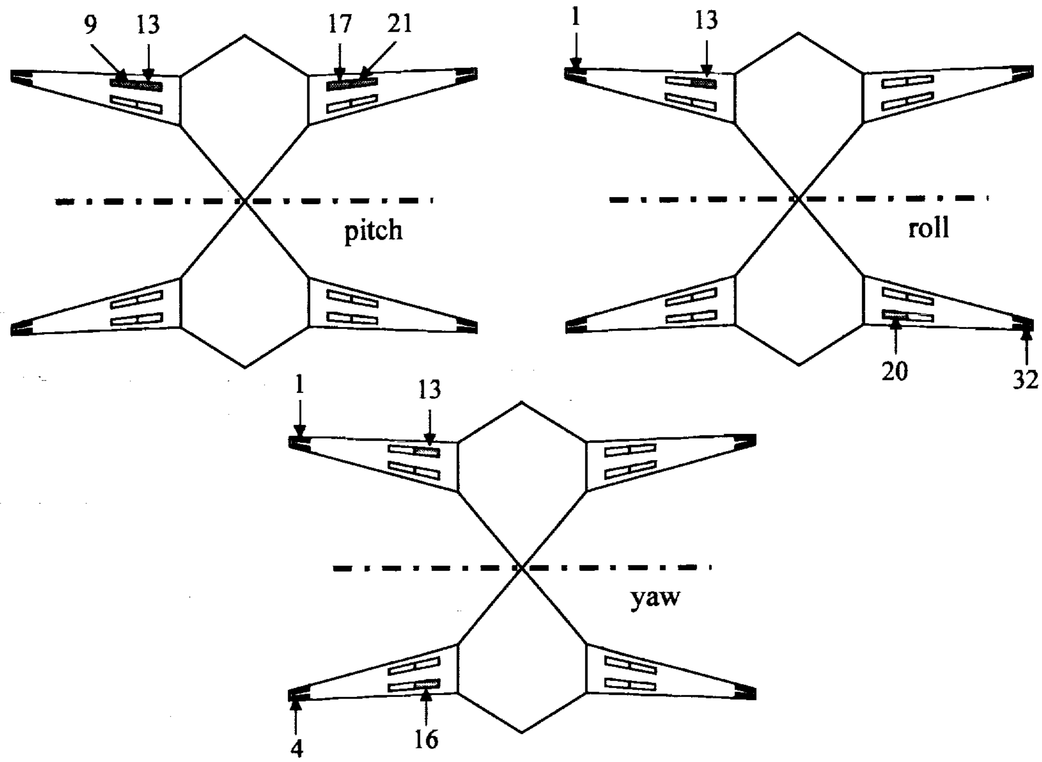


**Fig. 22 UAV combined moment problem result showing "on" actuator locations for the pitch, roll, and yaw maneuver "on" locations, 32 actuator locations.**

The fitness history plots corresponding to the above placement result are shown in Fig. 23. This example required 33 generations to invoke the stopping criterion. The best design of 9 actuators first occurred in generation 29. At the end of the GA run, the population contained other feasible placement designs using nine or more actuators, so a designer would be able to apply additional criteria to select the most appropriate placement scheme.

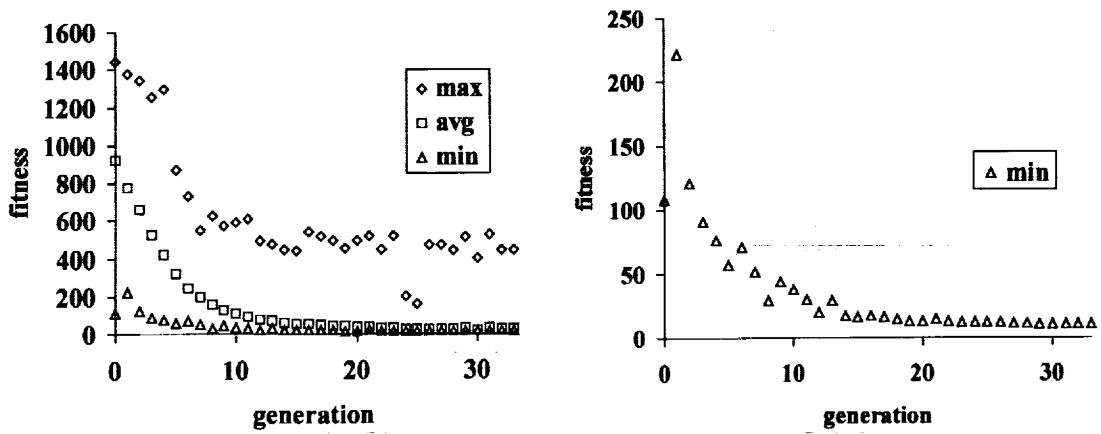


**Fig. 23 Fitness history with maximum, minimum, and average fitness (left) and minimum fitness only (right) for UAV problem, 32 possible actuator locations.**

The total CPU time for this problem was 64 hours; this UAV problem required more time than the wing model with 32 possible actuator locations. This time discrepancy is not due to the aerodynamic modeling. The UAV has a total of 2,352 panels in its PMARC model, and the wing model has 2,400 panels. This similarity would suggest that analysis time for a UAV actuator placement should be roughly equivalent to the analysis time of a wing model. Because of the camber, taper, and twist in the UAV's wing, the UAV placement problem is much more complicated than the wing problem. Without the geometric symmetry of the NACA 0015 section wing, fewer feasible (uncoupled moment) placement designs exist in the UAV design space. This lower number of feasible placements and the accompanying increase in complexity are evident in Fig. 23. In the early generations of the UAV problem, the maximum, average, and minimum fitness values are much higher in the early generations than they were for the 32-location simple wing model (see Fig. 13 for comparison). In fact, the minimum fitness value does not drop below 32, which would be the fitness value for a feasible design using all possible actuator locations, until the eighth generation. Based on this, it is reasonable to assume that no feasible UAV placements are found until sometime around generation 14.

In addition to complicating the design space, the top-to-bottom geometric asymmetry in the UAV model presents an issue for extending the three moment results to all six moments needed to full flight control. Six additional actuator locations provide all moments for the design shown in Fig. 22. For roll and yaw, the magnitude of $c_l$ and $c_n$ will be the same in both directions - only the sign is changed, because the UAV has left-to-right symmetry. However, when turning on upper surface actuators to provide the pitch up moment, the magnitude of $c_m$ will not be the same. This is not an inherent difficulty for the GA method; it would be best handled by determining which direction of pitch requires the largest magnitude moment and then using this as the limit value for the constraints. For the GA runs conducted here, this was not attempted.

The example described above required 33 generations to reach the stopping criterion, and the GA required an average of about 34 generations to complete a run for the UAV model. With 32 possible actuator locations, there are 65,536, possible actuator schemes that would each require three PMARC analyses in an enumerative approach, but the GA evaluated only 6,336 actuator placements over 33 generations in order to locate several feasible designs 10-actuator designs in the final population. For the UAV problem, as for the simple wing problem, the computational expense of the GA is far lower than that required by an exhaustive search.

The results of the GA application to the UAV model show that this is a practical and comparably efficient means of determining the minimum number and placement of actuators on a realistic aircraft model. The selection of possible actuator locations was somewhat arbitrary; an attempt was made to select locations on the wing close to locations used by traditional control surfaces. Similarly, the number of locations (32) in the investigation was also somewhat arbitrary. This actuator placement problem for the UAV could easily be made more complex by increasing the number of actuators and/or re-defining the locations of the actuators. Based on how well the GA approach scaled up as the number of actuator locations was increased on the simple wing model, the approach should perform similarly on more complicated placement problems using an aircraft aerodynamic model.

## CONCLUSIONS

The successful results of this research continued built upon previous research for smart actuator placement. The effort described here demonstrates that a genetic algorithm optimization approach is an effective method for selection of a minimum number of actuator locations on an aircraft to provide uncoupled aerodynamic moments about all three aircraft body axes. The binary coding of the GA allows for discrete optimization in this problem, which is difficult or impossible to implement in other optimization techniques. The GA approach could use nearly any aerodynamic analysis, and any smart actuator or effector can be modeled as long as a computational representation exists, like the surface blowing / suction approach used here.

The combined moment problem statement developed in this work is appropriate for actuator placement. This combination of placements in one problem statement can easily be posed using a chromosome that represents active actuator locations for each of the three moments. In this work, an array was used to represent these locations. Because three maneuvers are desired, each placement design evaluated by the GA requires three PMARC analyses. Posing the problem using three specific aerodynamic moments defines a single direction for each maneuver (e.g. nose-up pitch), so the GA-generated placement scheme can perform this prescribed maneuver, but not the opposite direction. Maneuver symmetry can be used to determine which additional actuators are required to perform these opposite direction maneuvers. Finally, the results generated for the combined moment problem met the constraints; the resulting placements for each of the three maneuvers satisfied or exceeded the limit on the desired moment while producing zero (in nearly every case) moment about the other two body axes. In some instances, the placements were somewhat non-intuitive, suggesting that the GA may discover placement schemes that would not have been considered by a designer.

Increasing the number of possible actuator locations on the simple wing model allowed for an investigation of how the GA approach for actuator placement performs for varying problem sizes. As the number of possible actuator locations increased, the GA was still able to generate placement solutions that minimized the number of on actuators needed and satisfied specified constraints on the aerodynamic moments. The increasing number of actuator locations required an increase in the number of bits used to represent placement designs in the genetic algorithm. With appropriate adjustments in population size and mutation rate to accommodate different chromosome lengths, the advantages the GA has over an enumerative search were illustrated. For the largest problem attempted, which had 64 possible locations for on actuators, the GA required an average of 53,914 PMARC analyses. This is still computationally intensive, but compares extremely well with the $2.4\times10^{24}$ analyses that would be required for a comprehensive enumerative search.

Research preceding this effort and the first tasks of this effort used a geometrically simple wing model to investigate issues associated with the actuator placement problem. In the later portion of the research effort described in this document, the genetic algorithm approach determined actuator placements to provide flight control moments for a high-altitude unmanned aerial vehicle concept. Representing actuators with normal surface velocities in the panel code PMARC followed the approach developed for the simple wing model; this technique appears to adequately model the effects of active actuators on the aircraft model. The GA successfully determined actuator placement designs that minimized the number of active actuators and satisfied aerodynamic moment constraints, even with the geometric complexity of the UAV concept, which decreases the number of feasible placement designs in the design space. The computational effort required to determine actuator placements on the UAV is far less than would be required of an enumerative approach.

This approach was successful for actuator placement on a simple wing model with increasing numbers of actuator locations and then was successful for actuator placement on an aircraft configuration. Because of this, the genetic algorithm appears to be a very useful tool that will assist designers pursuing flight control of morphing aircraft with different configurations and larger numbers of possible actuator locations.

## REFERENCES

[1] Wlezien, R. W., Horner, G. C., McGowan, A. R., Padula, S. L., Scott, M. A., Silcox, R. H., and Simpson, J. O., "The Aircraft Morphing Program," AIAA 98-1927, 39th AIAA/ASME/ASCE/AHS/ASC Structures, Structural Dynamics, and Materials Conference, Apr. 1998.

[2] Scott, M. A., Montgomery, R. C., and Weston, R. P., "Subsonic Maneuvering Effectiveness of High Performance Aircraft Which Employ Quasi-Static Shape Change Devices," 36th SPIE 5th Annual International Symposium on Smart Structures and Materials, San Diego, CA, Mar. 1-6, 1998.

[3] Lachowicz, J.T., Yao, C.S., and Wlezien, R.W., "Scaling of an Oscillatory Flow Control Actuator," AIAA 98-0330, 36th Aerospace Sciences Meeting & Exhibit, Reno, NV, Jan.12-15, 1998.

[4] Cook, A. M., and Crossley, W. A., "Genetic Algorithm Approaches to Smart Actuator Placement for Aircraft Flight Control," AIAA 2000-1582, 41st AIAA/ASME/ASCE/AHS/ASC Structures, Structural Dynamics and Materials Conference and Exhibit, April 3-6, 2000.

[5] Crossley, W. A., and Cook, A. M., "Genetic Algorithm Approaches for Actuator Placement," Final Summary of Research, NASA Grant NAG 1-2119, Sep. 2000.

[6] Goldberg, D. E., *Genetic Algorithms in Search, Optimization, and Machine Learning*, Addison-Wesley, Reading, MA, 1989.

[7] Ashby, D. L., Dudley, M. R., Iguchi, S. K., Browne, L., and Katz, J., "Potential Flow Theory and Operation Guide for the Panel Code PMARC_12," NASA Ames Research Center, Moffett Field, CA, Dec. 1992.

[8] Drela, M., "XFOIL: An Analysis and Design System for Low Reynolds Number Airfoils," *Proceedings of the Third International Conference on Aerodynamics at Low Reynolds Numbers*, Springer-Verlag, New York, 1989, pp. 1-12.

[9] Williams, E. A., and Crossley, W. A., "Empirically-Derived Population Size and Mutation Rate Guidelines for a Genetic Algorithm with Uniform Crossover," *Soft Computing in Engineering Design and Manufacturing*, P. K. Chawdhry, R. Roy and R. K. Pant (editors), Springer-Verlag, 1998, pp. 163-172.

[10] Helms, J., Prock, B., Kayir, T., Remson, A., Martin, E., and St. John, C., "OSCAR: Omni-directional SensorCraft for Aerial Reconnaissance," AAE 451 Senior Design Class, Purdue University School of Aeronautics and Astronautics, West Lafayette, IN, Apr. 2000.

## INVENTIONS

No inventions were developed as a result of this research.

## BIBLIOGRAPHY

Publications resulting from this research are listed below.

Cook, A. M. and Crossley, W. A., "Investigating a Genetic Algorithm Approach to Place Smart Actuators for Aircraft Maneuvering," AIAA Paper 2001-0924, 39th AIAA Aerospace Sciences Meeting and Exhibit, Reno, NV, Jan. 2001.

Cook, A. M. and Crossley, W. A., "Smart Actuator Placement for Aircraft Flight Control via a Genetic Algorithm Approach," in preparation for submittal to *Journal of Aircraft*, summer 2001.